

Experimental Comparison of Complementary Filter and Kalman Filter Design for Low-Cost Sensor in Quadcopter

H.-Q.-T. Ngo, T.-P. Nguyen, V.-N.-S. Huynh, T.-S. Le and C.-T. Nguyen

Abstract— Most of quadcopter operate in the outdoor environment where is often complex and unpredicted. In order to control the quadcopter in unknown outdoor environment, it should be designed an excellent filter to estimate complete state vector which illustrates the movement of rigid body. In this paper, two filters such as Complementary and Kalman are investigated to compare the performance. Quadcopter collect only measurements from a low-cost inertial measurement unit, IMU-MPU6050. The raw data is put into filter to estimate the state vector in system. In the simulations, these filters are studied to implement in the model of quadrotor. Later, the hardware platform of quadcopter is built to denote experimental results in order to validate the effective design of Complementary filter and Kalman filter in quadcopter.

Keywords— Quadcopter, Complementary, Kalman

I. INTRODUCTION

Although quadcopters become more popular not only in affordable applications but also in academic research because of its easy and cheap design, it is still active topic for researchers during many years. State estimation is addressed as one of traditional problems in quadcopter. There are large literatures on filtering techniques to estimate parameters of quadcopter. Many advanced filter, such as particle filter, are computational burden and suitable for powerfull processor in mainboard. Two common methods that are often used are Kalman filter and Complementary filter due to its frequency filtering characteristics in linear system [1]. Various studies focus on Kalman filter [2, 3, 4] in the flight control field. For the air vehicle attitude estimation, authors [5] modify the standard Kalman filter to update measurements. The estimated values are calculated using a multiplicative extended Kalman filter. The estimation receive data from accelerometers, gyroscopes and GPS. Researchers in [6] proposed an unscented Kalman filter using the three-axis attitude determination algorithm as the observer. It works efficiently, but needs computational power considerably. This filter is also used to track the motion [7, 8, 9]. The filter processes data from small inertial/magnetic sensor.

However, it is difficult to apply this filter robustly [10]. In recent work, many practitioners use two complementary filters, i.e. direct complementary filter and passive complementary filter, to obtain high quality attitude extraction and gyros bias estimation. In this approach, both filters can be explicitly expressed in quaternion form for easy

Ha Quang Thinh Ngo is with Bach Khoa University (BKT), Ho Chi Minh city, Vietnam (phone: +84-8-3868-8611; fax: +84-8-3865-3823, e-mail: nhqthinh@hcmut.edu.vn).

Thanh Phuong Nguyen is with Ho Chi Minh University of Technology (HUTECH), Ho Chi Minh city, Vietnam.

Tan Sang Le, Van Ngoc Son Huynh and Chi Tong Nguyen are students in Bach Khoa University (BKT), Ho Chi Minh city, Vietnam.

implementation. Unfortunately, data from accelerometer is not excellent to estimate the gravitational direction if dynamics of air vehicle is large enough.

In this paper, Kalman filter and Complementary filter are implemented in quadcopter to visualize the performance. The key contribution is to build a routine of filtering selection technique. The rest of this article is structured as following. Section II performs the implementation of low-cost IMU-MPU6050 sensor. In Section III, the contents focus on theory of Kalman filter and Complementary filter basically. Later, modeling analysis of quadcopter is presented in Section IV. Then, several experiments in Section V is setup to validate our contributions. In Section VI, conclusions are carried out.

II. IMPLEMENTATION OF IMU-MPU6050

A. Estimated Orientation

MPU6050 is calibrated to center of gravity (CoG) of system. The rotation matrix of system:

$$R_{xyz}(\Phi, \theta, \psi) = R_z(\psi) R_y(\theta) R_x(\Phi) \quad (1)$$

$$= \begin{bmatrix} c\theta c\Psi & -c\Phi s\Psi + s\Phi s\theta c\Psi & s\Phi s\Psi + c\Phi s\theta c\Psi \\ c\theta s\Psi & c\Phi c\Psi + s\Phi s\theta s\Psi & -s\Phi c\Psi + c\Phi s\theta s\Psi \\ -s\theta & s\Phi c\theta & c\Phi c\theta \end{bmatrix}$$

Where Φ, θ, Ψ are roll, pitch and yaw angles respectively

Consider that R_1 is attached to earth inertial frame, R_2 parallel to R_1 and is placed at the CoG of system, R_3 is attached to the body of system and also placed at CoG of it.

The angular velocity of system (R_3):

$$\text{gyroRate} = \Omega = (\Omega_{x3}, \Omega_{y3}, \Omega_{z3}) \quad (2)$$

where

$$\begin{bmatrix} \Omega_{x3} \\ \Omega_{y3} \\ \Omega_{z3} \end{bmatrix} = \begin{bmatrix} 1 & 0 & -\sin\theta \\ 0 & \cos\Phi & \sin\Phi \cos\theta \\ 0 & -\sin\Phi & \cos\Phi \cos\theta \end{bmatrix} \begin{bmatrix} \dot{\Phi} \\ \dot{\theta} \\ \dot{\Psi} \end{bmatrix} \quad (3)$$

Euler angle is small, therefore, equation (3) can be rewritten as:

$$\begin{bmatrix} \Omega_{x3} \\ \Omega_{y3} \\ \Omega_{z3} \end{bmatrix} \approx \begin{bmatrix} \dot{\Phi} \\ \dot{\theta} \\ \dot{\Psi} \end{bmatrix} \quad (4)$$

B. Estimated Acceleration

Assume that the system is attached by a linear acceleration a_r and placed in gravitational acceleration. R is rotation matrix.

$$Acc = \begin{bmatrix} Acc_x \\ Acc_y \\ Acc_z \end{bmatrix} = R(g - a_r) \quad (5)$$

Consider that linear acceleration is small ($a_r \approx 0$). MPU6050 is placed its z axis along with gravitational acceleration.

$$Acc = \begin{bmatrix} Acc_x \\ Acc_y \\ Acc_z \end{bmatrix} = R \times g = R \begin{bmatrix} 0 \\ 0 \\ 1 \end{bmatrix} \quad (6)$$

Euler angles can be estimated from roll, pitch and yaw value of sensor.

$$R_x(\Phi) = \begin{bmatrix} 1 & 0 & 0 \\ 0 & \cos \Phi & \sin \Phi \\ 0 & -\sin \Phi & \cos \Phi \end{bmatrix} \quad (7)$$

$$R_y(\theta) = \begin{bmatrix} \cos \theta & 0 & -\sin \theta \\ 0 & 1 & 0 \\ \sin \theta & 0 & \cos \theta \end{bmatrix} \quad (8)$$

$$R_z(\Psi) = \begin{bmatrix} \cos \Psi & \sin \Psi & 0 \\ -\sin \Psi & \cos \Psi & 0 \\ 0 & 0 & 1 \end{bmatrix} \quad (9)$$

Then, from equation (6), we obtain the following.

$$R_{xyz} \times \begin{bmatrix} 0 \\ 0 \\ 1 \end{bmatrix} = R_x(\Phi) \times R_y(\theta) \times R_z(\Psi) \times \begin{bmatrix} 0 \\ 0 \\ 1 \end{bmatrix} \quad (10)$$

$$= \begin{bmatrix} -\sin \theta \\ \cos \theta \sin \Phi \\ \cos \theta \cos \Phi \end{bmatrix} \quad (11)$$

It means that the values from sensor can be achieved by these parameters.

$$\frac{Acc}{\|Acc\|} = \begin{bmatrix} -\sin \theta \\ \cos \theta \sin \Phi \\ \cos \theta \cos \Phi \end{bmatrix} \quad (12)$$

From above equation, roll and pitch angle are calculated.

$$\Phi_{xyz} = \arctan \left(\frac{Acc_y}{Acc_z} \right) \quad (13)$$

$$\theta_{xyz} = \arctan \left(\frac{-Acc_x}{\sqrt{Acc_y^2 + Acc_z^2}} \right) \quad (14)$$

III. FILTERS DESIGN FOR MPU6050

The role of gyroscope is to measure accurately and less noisy if external forces impact to system. However, based on the calculation by integral factor, error is cumulative over time and measurements tend to be drifted, not return to 0 even system is in its original point. Hence, gyroscope's values are only reliable in short-term. Due to MEMS structure of accelerometer, it is sensitive to vibrate when external forces appear. Accelerometer cannot calculate yaw angle and results aren't drifted over time because of lacking of integration. These values are suitable for a long-time period. Before using the filter, sensor is needed to reduce its maximum vibration by placing additional spacers separating the device from frame for damping and vibrationless. To lessen the amplitude of noise at high frequency which effects to the raw data, it is necessary to apply the built-in low-pass filter in MPU6050 with cutoff frequency of accelerometer and gyroscope that are 44Hz and 42Hz correspondingly.

A. Design of Complimentary filter

To handle the drifted phenomenon in gyroscope and reduce high frequency noise from accelerometer, Complementary filter is applied to estimate the angle based on the change of speed from gyroscope. Then, it is combined with angle from accelerometer as Fig. 1. Assume that with small angle, the estimated roll value (Φ) and the estimated pitch value (θ) are determined respectively.

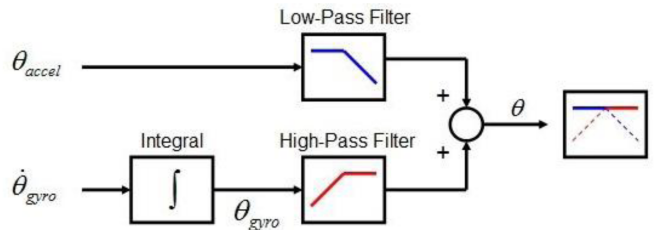


Figure 1. Scheme of Complementary filter

$$\Phi_{estimate}(n) = \Phi(n-1) + \Delta\Phi \approx \Phi(n-1) + \Omega_{x3} \quad (15)$$

$$\Phi(n) = \gamma \Phi_{estimate}(n) + (1-\gamma) \Phi_{accelerometer}(n) \quad (16)$$

$$\theta_{estimate}(n) = \theta(n-1) + \Delta\theta \approx \theta(n-1) + \Omega_{y3} \quad (17)$$

$$\theta(n) = \gamma \theta_{estimate}(n) + (1-\gamma) \theta_{accelerometer}(n) \quad (18)$$

$$0.5 \leq \gamma \leq 1$$

It can be seen clearly that quality of Complementary filter depends mainly on parameter γ . Output signal from this filter has a delay (mostly due to low-pass filter of accelerometer and high-pass filter from gyroscope). The more γ value is

close to 1, the better quality this filter has. But the convergent time is long when sensor is quickly changed. Yaw angle cannot infer directly from accelerometer, so currently we will use value inferred from gyroscope and accept the drifted phenomenon. This problem will be solved when using additional magnetic sensor.

B. Design of Kalman Filter

Kalman filter, as they are applied in navigation systems, are based on Complementary filtering principle. The basic block diagram is given in Fig. 2. The inputs of this filter include angle (x) and angular velocity (\dot{x}) which are described as following.

$$X_k = \begin{bmatrix} x \\ \dot{x} \end{bmatrix} \quad (19)$$

Therefore, the system state at time k is determined from the state at time k-1.

$$X_k = AX_{k-1} + BU_{k-1} + \omega_k \quad (20)$$

U_k is the vector containing control inputs. A is the state transition matrix which is applied the effect of each system state X_{k-1} on the system state X_k . B is the control input matrix which is applied the effect of each control input parameter in the vector U_k . ω_k is the process noise terms for each parameter in the state vector. The process noise is assumed to be drawn from a zero mean multivariate normal distribution N with covariance given by $P(\omega) \sim N(0, Q_k)$.

By some measured methods, at time k, an observation Z_k of the true state X_k is made according to.

$$Z_k = HX_k + V_k \quad (21)$$

H is the transformation matrix that maps the state vector parameters into the measurement domain. V_k is the observed noise which is assumed to be zero mean Gaussian white noise with covariance given by $P(V) \sim N(0, R_k)$.



Figure 2. Scheme of Kalman filter

Q_k and R_k are half-defined positive symmetric matrix representing for the process and measurement noise. The quality of Kalman filter depends on Q_k and R_k . However, the ratio Q_k / R_k plays more important role in the filter. The smaller the ratio is ($R_k \rightarrow Q_k$), the later the fluctuation amplitude of filter signal is. Otherwise, the larger the ratio is ($R_k \rightarrow 0$), the greater the fluctuation amplitude is and the shorter the delay time as well as the convergent time is.

IV. KINEMATICS AND DYNAMICS OF QUADCOPTER

A. Kinematics

Assume that quadcopter is a solid to be suffered by a force, that is total force of motors, and three moments, that turn it in roll, pitch and yaw angle. In Fig. 3, a model of quad-rotor is analyzed. Each motor provides a force T_i to lift up and a moment M_i to rotate quadcopter. The gravitational force is often toward center of the earth.

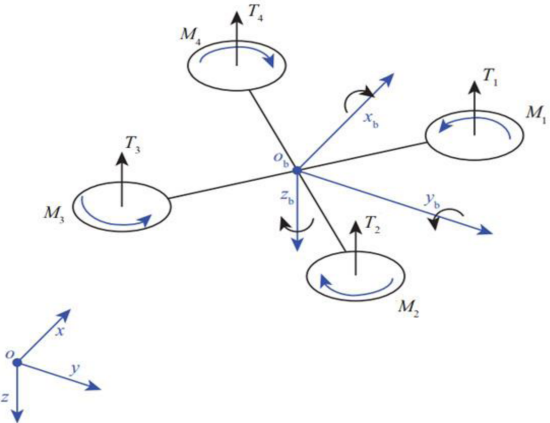


Figure 3. Analysis of Quadcopter Model

$\{E\} = [x_E, y_E, z_E]$, $\{B\} = [x_B, y_B, z_B]$ and $\{CS_v\} = [x_v, y_v, z_v]$ are the inertial frame, body frame and vehicle frame correspondingly. x, y, z which are alternately coordinates in centroid of quadcopter model, correspond alternately x_E, y_E, z_E axes in coordinate system $\{E\}$.

Matrix R_B^E : is rotation matrix from frame $\{B\}$ to frame $\{E\}$

$$R_{B(\Phi,\theta,\psi)}^E = \begin{bmatrix} c\theta c\psi & s\Phi s\theta c\psi - c\Phi s\psi & c\Phi s\theta c\psi + s\Phi s\psi \\ c\theta s\psi & s\Phi s\theta s\psi + c\Phi c\psi & c\Phi s\theta c\psi - s\Phi c\psi \\ -s\theta & s\Phi c\theta & c\Phi c\theta \end{bmatrix} \quad (22)$$

Matrix R_E^B : is rotation matrix from frame $\{E\}$ to frame $\{B\}$.

$$R_E^B(\Phi, \theta, \psi) = R_B^E(\Phi, \theta, \psi)^T \quad (23)$$

The relationship between position vector ξ^E in frame $\{E\}$ and linear velocity vector V^B in frame $\{B\}$ is shown as follows.

$$V^E = \dot{\xi}^E = \begin{pmatrix} \dot{x} \\ \dot{y} \\ \dot{z} \end{pmatrix} = R_B^E V^B \quad (24)$$

$$\begin{pmatrix} \dot{x} \\ \dot{y} \\ \dot{z} \end{pmatrix} = \begin{bmatrix} c\theta c\psi & s\Phi s\theta c\psi - c\Phi s\psi & c\Phi s\theta c\psi + s\Phi s\psi \\ c\theta s\psi & s\Phi s\theta s\psi + c\Phi c\psi & c\Phi s\theta c\psi - s\Phi c\psi \\ -s\theta & s\Phi c\theta & c\Phi c\theta \end{bmatrix} \begin{pmatrix} u \\ v \\ w \end{pmatrix} \quad (25)$$

Matrix T: is computed to show relationship between angular velocity vector ω^B in frame {B} and frame {E}.

$$\begin{pmatrix} p \\ q \\ r \end{pmatrix} = \begin{pmatrix} 1 & 0 & -s\theta \\ 0 & c\Phi & s\Phi s\theta \\ 0 & -s\Phi & s\Phi c\theta \end{pmatrix} \begin{pmatrix} \dot{\Phi} \\ \dot{\theta} \\ \dot{\psi} \end{pmatrix} \quad (26)$$

$$\begin{pmatrix} \dot{\Phi} \\ \dot{\theta} \\ \dot{\psi} \end{pmatrix} = \begin{pmatrix} 1 & s\Phi t\theta & c\Phi t\theta \\ 0 & c\Phi & -s\Phi \\ 0 & s\Phi / c\theta & c\Phi / c\theta \end{pmatrix} \begin{pmatrix} p \\ q \\ r \end{pmatrix} \quad (27)$$

From that, matrix T can be obtained.

$$T = \begin{pmatrix} 1 & s\Phi t\theta & c\Phi t\theta \\ 0 & c\Phi & -s\Phi \\ 0 & s\Phi / c\theta & c\Phi / c\theta \end{pmatrix} \quad (28)$$

B. Dynamics

In the Newton's second rule to the translational motion, we have equations [11].

$$m\ddot{x}^E = F^E \quad (29)$$

$$m.\dot{V}^E = F^E \quad (30)$$

$$m.(R.\dot{V}^B + \dot{R}.V^B) = R.F^B \quad (31)$$

$$m.(R.\dot{V}^B + R\omega^B \times V^B) = R.F^B \quad (32)$$

$$\dot{V}^B = -\omega^B \times V^B + \frac{F^B}{m} = \begin{pmatrix} rv - qw \\ pw - ru \\ qu - pv \end{pmatrix} + \frac{1}{m} \begin{pmatrix} f_x \\ f_y \\ f_z \end{pmatrix} \quad (33)$$

$$\begin{pmatrix} \dot{u} \\ \dot{v} \\ \dot{w} \end{pmatrix} = \begin{pmatrix} rv - qw \\ pw - ru \\ qu - pv \end{pmatrix} + \frac{1}{m} \begin{pmatrix} f_x \\ f_y \\ f_z \end{pmatrix} \quad (34)$$

$V^B = (u, v, w)^T$ and $\omega^B = (p, q, r)^T$. From Newton's law to rotational motion, we get:

$$\tau^B = J.\dot{\omega}^B + \omega^B \times (J.\omega^B) \quad (35)$$

$$\Rightarrow \dot{\omega}^B = \frac{\tau^B}{J} - \frac{\omega^B \times (J.\omega^B)}{J} \quad (36)$$

Consider that structure of quadcopter is symmetry and axes in {B} coincide with inertial axes of quadcopter.

$$\begin{pmatrix} \dot{p} \\ \dot{q} \\ \dot{r} \end{pmatrix} = \begin{pmatrix} qr \frac{I_{yy} - I_{zz}}{I_{xx}} \\ pr \frac{I_{zz} - I_{xx}}{I_{yy}} \\ pq \frac{I_{xx} - I_{yy}}{I_{zz}} \end{pmatrix} + \begin{pmatrix} \frac{\tau_\Phi}{I_{xx}} \\ \frac{\tau_\theta}{I_{yy}} \\ \frac{\tau_\psi}{I_{zz}} \end{pmatrix} \quad (37)$$

$$J = \begin{bmatrix} I_{xx} & 0 & 0 \\ 0 & I_{yy} & 0 \\ 0 & 0 & I_{zz} \end{bmatrix} \quad (38)$$

$$\omega^B \times (J.\omega^B) = \left(qr \frac{I_{yy} - I_{zz}}{I_{xx}}, pr \frac{I_{zz} - I_{xx}}{I_{yy}}, pq \frac{I_{xx} - I_{yy}}{I_{zz}} \right)^T \quad (39)$$

V. EXPERIMENTAL LABORATORY

In these experiments, MPU6050 is set-up on the drone and is supervised by host through GUI in Fig. 4. γ , for Complementary filter, varies from 0,95 to 0,99 and R, for Kalman filter, is 0,5~0,7 so that sensor achieves good performance. As a result, they are selected as the best suitable value ($\gamma=0,9996$, $R=0,5721$).

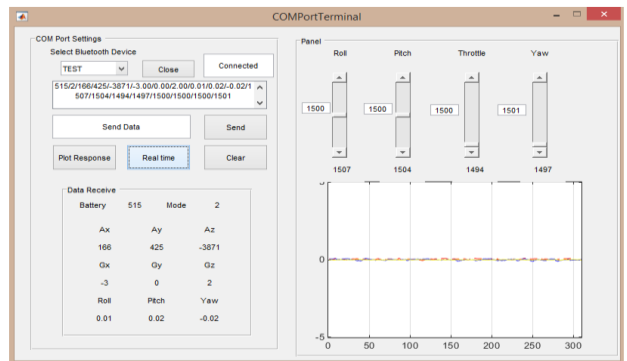


Figure 4. Graphical User Interface on host

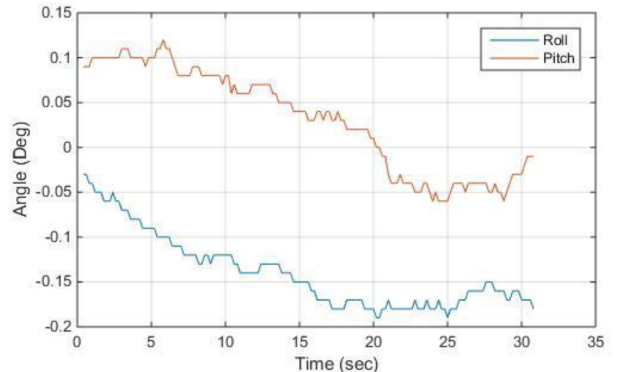


Figure 5. Performance of Roll and Pitch Angle by Complementary Filter

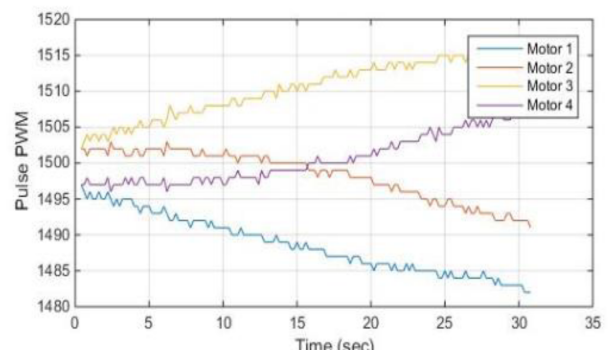


Figure 6. Performance of Speed by Complementary Filter

In Fig. 5 and Fig. 6, Complementary filter gets values of gyro as major factors and values of accelerometer as minor factors. Hence, the oscillation (caused by motors, propellers) that reflects into angles of accelerometer would not impact on the system so much. The estimated angle of Complementary filter is more stable than that of Kalman filter. Actually, it still exists the drift phenomenon (approximate $\pm 0.5^\circ$). In contrary, the performance of Kalman filter in Fig. 7 and Fig. 8 receives angles of accelerometer to estimate the real angle. It leads to the fact that this filter appreciates more precise values. However, the pulse modulation to each motor depends on the vibration of system.

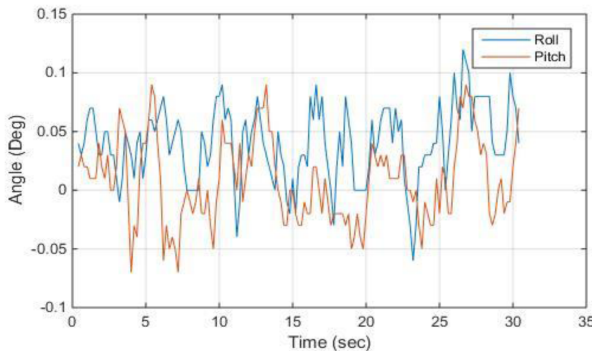


Figure 7. Performance of Roll and Pitch Angle by Kalman Filter

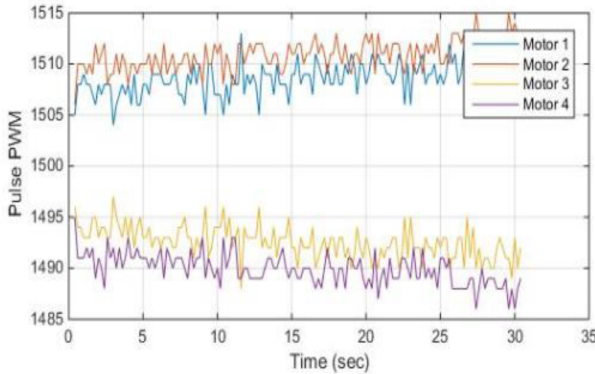


Figure 8. Performance of Speed by Kalman Filter

In order to examine the balancing capability on one axis, the experiment in Fig. 9 is built to investigate the hardware of system. This quadcopter is suspended on a stick and the controller try to keep the fixed angle such as 10, 30 and -35 degree. In Fig. 10 and Fig. 11, several angular and speed results are obtained by Kalman filter. The system is started testing at the 17s and balancing at the 40s. Later, a stick is turned to left the balancing point during 5s. Quadcopter retains the pre-determined angle from 45s.

Later, quadcopter is hung up by four ropes to assess the balancing ability on 6 DOF as shown in Fig. 12. The angular and speed test results are done by Complementary filter in Fig. 13 and Fig. 14. The overall system is activated at the 5s. After a few seconds, quadcopter is lifted from the ground and stabilized in this position. The similar test conditions are applied for Kalman filter in Fig. 15 and Fig. 16. Quad-rotor is able to hold the equilibrium with ± 3 degree although it suffers the external disturbances in outdoor environment.

From these results, it can be seen easily that Complementary filter is more superior than Kalman filter in this test case. In Fig. 17, quadcopter works well when the PID controller runs with the good tuning parameters based on the experiences such as $K_p=1.3$; $K_i=0.004$ and $K_D=18$.

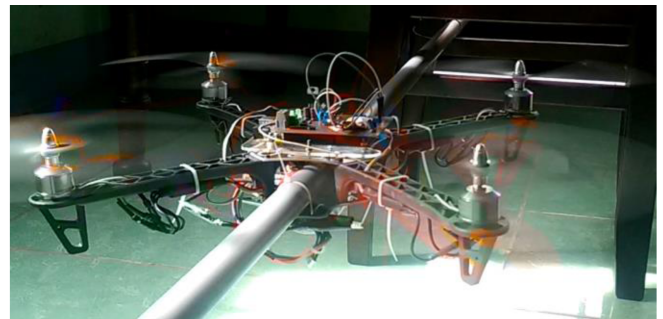


Figure 9. One-axis Balancing Test Case

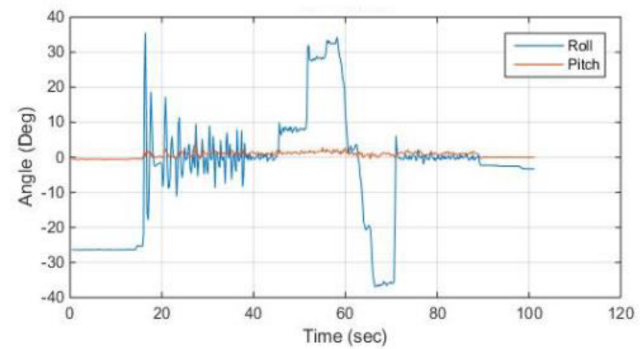


Figure 10. Angular Results by Kalman Filter on One Axis

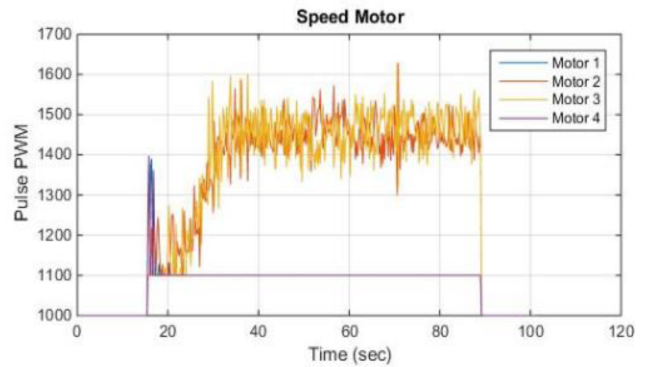


Figure 11. Speed Results by Kalman Filter For 4 Motors



Figure 12. 6 DOF Balancing Test Case

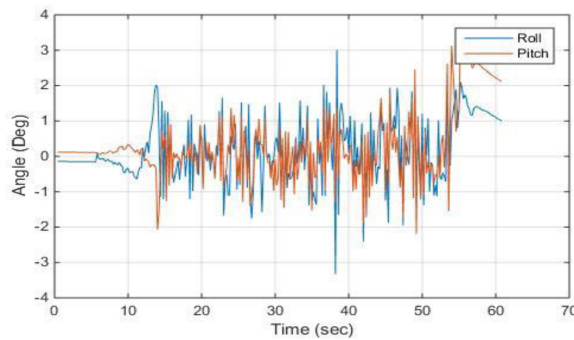


Figure 13. Angular Results on 6 DOF by Complementary Filter

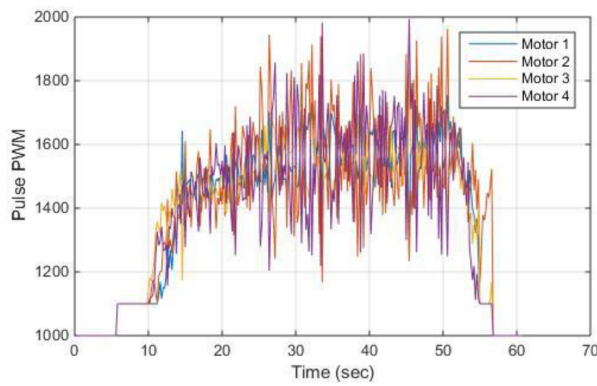


Figure 14. Speed Results on 6 DOF by Complementary Filter

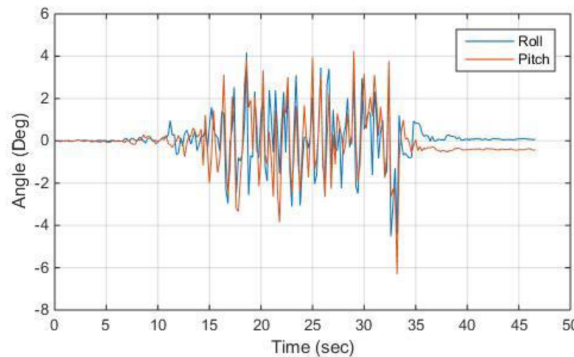


Figure 15. Angular Results on 6 DOF by Kalman Filter

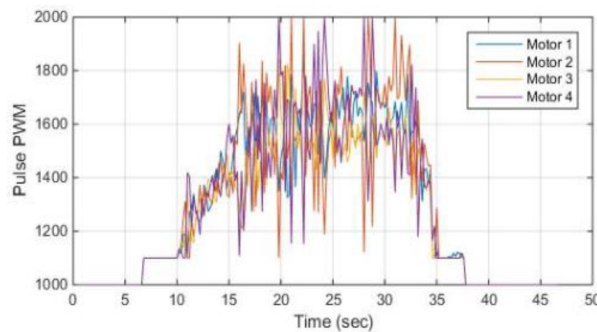


Figure 16. Speed Results on 6 DOF by Kalman Filter



Figure 17. Experimental Test in Outdoor Environment

VI. CONCLUSION

In this paper, an application of Complementary filter and Kalman filter in quadcopter is studied. The method to work and compute the output for IMU-MPU6050 is performed in order to insist on major factors in both filters. The kinematics and dynamics of quadrotor are analyzed to implement. Hardware and software design are completed to carry out several experimental results. From these outcomes, the effective filter is proposed for low-cost IMU-MPU6050 in the flight control technique.

REFERENCES

- [1] R. Mahony, T. Hamel and J.-M. Pflimlin, "Nonlinear complementary filters on the special orthogonal group," in *IEEE Trans. on Automatic Control*, vol. 53, no. 5, 2008, pp. 1203–1218.
- [2] D. Hetényi, M. Gótzy and L. Blázovics, "Sensor fusion with enhanced Kalman Filter for altitude control of quadrotors," in *IEEE 11th International Symposium on Applied Computational Intelligence and Informatics (SACI)*, 2016, pp. 413–418.
- [3] H. Beck, J. Lesueur, G.-C. Arcand, O. Akhrif, S. Gagné, F. Gagnon and D. Couillard, "Autonomous takeoff and landing of a quadcopter," in *International Conference on Unmanned Aircraft Systems (ICUAS)*, 2016, pp. 475–484.
- [4] K.-D. Sebesta and N. Boizot, "A real-time adaptive high-gain EKF, Applied to a quadcopter inertial navigation system," in *International IEEE Trans. On Industrial Electronics*, vol. 61, no. 1, 2014, pp. 495–503.
- [5] J. K. Hall, N. B. Knoebel and T. W. McLain, "Quaternion attitude estimation for miniature air vehicles using a multiplicative extended Kalman filter," in *IEEE on Position, Location and Navigation Symposium*, 2008, pp. 1230–1237.
- [6] H. G. De Marina, F. J. Pereda, J. M. Giron-Sierra and F. Espinosa, "UAV attitude estimation using unscented kalman filter and triad," in *IEEE Transactions on Industrial Electronics*, vol. 59, no. 11, 2012, pp. 4465–4474.
- [7] X. Yun and E. R. Bachmann, "Design, Implementation and Experimental Results of a Quaternion-based Kalman Filter for Human Body Motion Tracking," in *IEEE Transactions on Robotics*, vol. 22, no. 6, 2006, pp. 1216–1227.
- [8] H. Q. T. Ngo, Q. C. Nguyen and W. H. Kim, "Implementation of input shaping control to reduce residual vibration in industrial network motion system," *International Conference on Control, Automation and Systems*, Busan, Korea, 2015, pp. 1693–1698.
- [9] H. Q. T. Ngo, Q. C. Nguyen and T. P. Nguyen, "Design and Implementation of High Performance Motion Controller for 2-D Delta Robot," *Seventh International Conference on Information Science and Technology*, Da Nang, Vietnam, 2017, pp. 129–134.
- [10] R. Mahony, T. Hamel and J.-M. Pflimlin, "Complementary filter design on the special orthogonal group SO(3)," in *Proc. Of 44th IEEE Conf. On Decision and Control and the European Control Conference*, 2005, pp. 1477–1484.
- [11] V. K. Tripathi, L. Behera and N. Verma, "Design of sliding mode and backstepping controllers for a quadcopter", in *39th National Systems Conference*, 2015.